How to cite: *Angew. Chem. Int. Ed.* **2023**, *62*, e202310672
doi.org/10.1002/anie.202310672

Xylene Separation | Hot Paper

Separating Xylene Isomers with a Calcium Metal-Organic Framework

Liang Yu[+], Jian Zhang[+], Saif Ullah[+], Jinze Yao, Haoyuan Luo, Jiajin Huang, Qibin Xia, Timo Thonhauser, Jing Li, and Hao Wang**

Abstract: The purification of p-xylene (pX) from its xylene isomers represents a challenging but important industrial process. Herein, we report the efficient separation of pX from its ortho- and meta- isomers by a microporous calcium-based metal–organic framework material (HIAM-203) with a flexible skeleton. At 30 °C, all three isomers are accommodated but the adsorption kinetics of o-xylene (oX) and m-xylene (mX) are substantially slower than that of pX, and at an elevated temperature of 120 °C, oX and mX are fully excluded while pX can be adsorbed. Multicomponent column breakthrough measurements and vapor-phase/liquid-phase adsorption experiments have demonstrated the capability of HIAM-203 for efficient separation of xylene isomers. *Ab initio* calculations have provided useful information for understanding the adsorption mechanism.

Xylene isomers are critical organic raw materials in chemical industry for various end uses. In particular, pX is used as a starting chemical for the production of polyesters and polyamides.[1] The separation of pX from mixtures of xylene isomers is a crucial step for producing pX with high purity for further uses.[2] However, separation of the three xylene isomers with very similar physicochemical properties is a daunting challenge that has been listed as one of the seven chemical separations to change the world (Table S1).[3] Because of their nearly-the-same boiling points, efficient separation of xylene isomers through traditional distillations is not practical, and the dominant separation methods currently applied in industry are crystallization and adsorption.[4] Purification of pX via crystallization suffers from low recovery, thus adsorption-based separation is more widely used. However, the relatively low selectivity of the currently used adsorbents (e.g. KBaX) has limited the overall efficiency of the adsorption-based technology.[5] Thus, developing novel porous solids with high adsorption selectivity for xylene isomers represents a major and urgent task for pX production.

In this context, metal–organic frameworks (MOFs) hold promises for the selective adsorption of xylene isomers in light of their structural diversity and tunable pore dimension compared to traditional organic and inorganic adsorbents. Over the past several years, a number of MOFs have been evaluated for the separation of xylene isomers, through various experimental techniques including single component adsorption, multicomponent column breakthrough, multi-component vapor/liquid adsorption, and gas chromatography.[6–7] Thermodynamically discrimination of xylene isomers through tailoring MOF adsorption sites or structural flexibility has been demonstrated by Xing,[8] Zhang,[9] Long and co-workers.[2] Kinetic separation of xylenes has also been achieved through precise refinement of the pore size of MOFs by Yang, Fedin and co-workers.[3,10] Recently, Bao, Li, and co-workers demonstrated the temperature-dependent splitting of xylene isomers by a stacked one-dimensional (1D) coordination polymer.[4] Overall, adsorbent materials that can fully separate the needed pX from oX and mX remain scarce.[11]

Here, we show the substantial adsorption of pX and full exclusion of its xylene isomers by a calcium-chloranilate framework (HIAM-203) at industrially relevant temperature (120 °C). HIAM-203 exhibits temperature-dependent adsorption behavior toward the three xylene isomers. It can accommodate all three isomers at 30 °C but with different kinetics while at 120 °C only pX is adsorbed, leading to high pX/mX and pX/oX selectivities and efficient separation capability that has been validated by various experimental methods.

HIAM-203 was prepared through solvothermal reactions following reported procedures.[12] Uniform purple strip-shaped crystals were obtained by heating a mixture of $CaCl_2$ and chloranilic acid in ethanol (95 %) at 150 °C for 2 days (Figure S1). The phase purity of the product was confirmed by powder X-ray diffraction (PXRD) analysis (Figures S2). The crystal structure of HIAM-203 was re-visited using data collected at 393 K, which gave the same results to the previous structure determined from data collected at 193 K

[*] L. Yu,[+] J. Yao, H. Luo, J. Huang, Prof. Q. Xia
School of Chemistry and Chemical Engineering, South China University of Technology
Guangzhou 510640 (P. R. China)
E-mail: qbxia@scut.edu.cn

L. Yu,[+] Dr. J. Zhang,[+] Prof. J. Li, Prof. H. Wang
Hoffmann Institute of Advanced Materials, Shenzhen Polytechnic
7098 Liuxian Blvd., Nanshan District, Shenzhen 518055 (P. R. China)
E-mail: wanghao@szpt.edu.cn

Dr. S. Ullah,[+] Prof. T. Thonhauser
Department of Physics and Center for Functional Materials, Wake Forest University
Winston-Salem, NC 27109 (USA)

Prof. J. Li
Department of Chemistry and Chemical Biology, Rutgers University
123 Bevier Road, Piscataway, NJ 08854 (USA)

[+] These authors contributed equally to this work.

(Table S2).[13] HIAM-203 is built on arrays of octahedrally coordinated Ca^{2+} (omitting coordinated terminal ethanol) which are further connected through chloranilate linkers (Figure 1). The overall structure features a three-dimensional (3D) framework with 1D rhombic channels decorated by chlorine atoms from the chloranilate linkers. Thermogravimetric analysis (TGA) revealed the solvents in the channels of HIAM-203 could be completely removed upon heating at 150 °C or above (Figure S3). HIAM-203 is stable in various organic solvents including acetonitrile, isopropanol, dichloromethane, and xylenes (Figure S4–S5). N_2 adsorption-desorption isotherm at 77 K displayed a Type I profile, yielding a BET surface area of 480 m^2/g and a pore volume of 0.21 cm^3/g, and the calculated pore size distribution curve is centered at 6 Å (Figure S6–S7). It should be noted that HIAM-203 undergoes a structural change upon solvent removal, however, the activated structure returns readily back to the original structure after being immersed in organic solvents (Figure S2, Figure S4–S5).

To investigate the adsorption and separation capability of HIAM-203 towards xylene isomers, single-component vapor adsorption isotherms of pX, oX, and mX were collected at various temperatures including 30, 60, 90, 120 and 150 °C (Figure 2a-2c and Figures S8–S11). The adsorption behavior is highly temperature-dependent, particularly for oX and mX. At 30 °C, the adsorption of all three xylene isomers displayed a typical Type I profile, and the saturated adsorption capacities for the three isomers were similar assuming sufficient equilibrium time was given (199, 200, 159 mg/g for pX, oX, and mX, respectively, Figure S8). However, the adsorption amounts of oX and mX decreased dramatically as temperature increased. At 120 °C or above, HIAM-203 adsorbed essentially no oX or mX, but it accommodated substantial amount of pX (151 mg/g at 120 °C and 142 mg/g at 150 °C, Figure 2d and Figure S11).

Adsorption rates of the three isomers were also measured to evaluate the adsorption kinetics. While all three xylene isomers were adsorbed substantially by HIAM-203 at 30 °C, their adsorption kinetics differed significantly (Figure S12). It displayed a fast adsorption rate for pX, reaching adsorption equilibrium within 40 minutes with a dynamic adsorption capacity of 170 mg/g. In contrast, substantially slower adsorption rates for oX and mX were observed, with no signs of approaching equilibrium after several hours. These results indicated that the diffusion rates of xylene isomers in HIAM-203 were distinctly different. As such, HIAM-203 can potentially distinguish the isomers through kinetically controlled mechanism at 30 °C. Adsorption rates at 120 °C showed that adsorption equilibrium was reached within ≈25 minutes for pX, and no notable uptake was observed for oX or mX, confirming the fact that they were fully excluded by the adsorbent (Figure 2e). These results verified that HIAM-203 is capable of separating xylene isomers via size exclusion at 120 °C.

To quantitatively evaluate the adsorption selectivity of HIAM-203, ideal adsorbed solution theory (IAST) was applied to calculate pX/oX and pX/mX selectivities using the adsorption isotherms at 120 °C. The calculated pX/oX

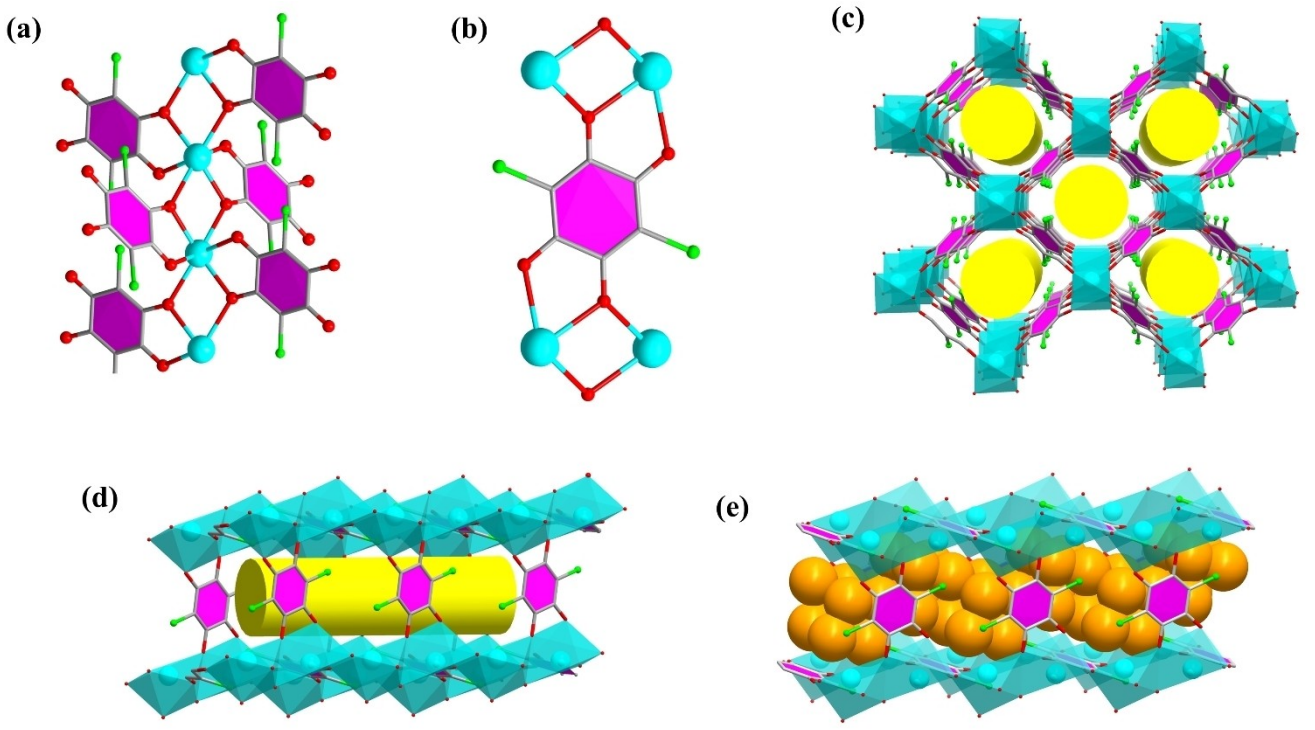

Figure 1. Crystal structure of HIAM-203. (a) Coordination environment of Ca^{2+}. (b) Each chloranilate ligand connects with four different Ca^{2+} (c, d) 3D structure of HIAM-203 showing the 1D open rhombic channels. (e) The shape of the 1D channels is outlined by the simulated adsorption of helium atoms. Color Scheme: Ca: cyan, O: red, C: gray, Cl: green, He (CPK display): Orange.

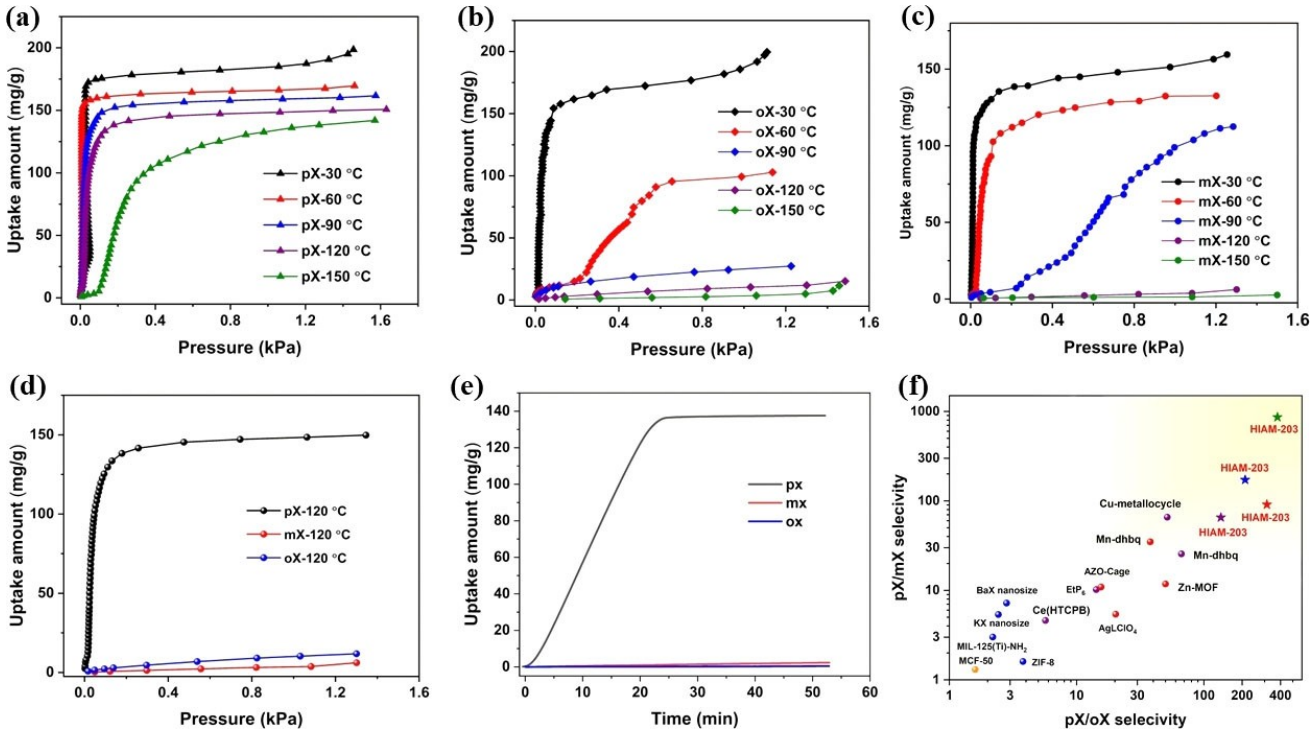

Figure 2. Single-component vapor adsorption isotherms of (a) pX, (b) oX and (c) mX on HIAM-203 at 30, 60, 90,120 and 150 °C. (d) Comparison of the adsorption of pX, oX and mX at 120 °C. (e) Adsorption kinetics of pX, oX and mX at 120 °C. (f) The pX/oX and pX/mX selectivities of HIAM-203 and representative adsorbents (For the reported adsorbents, only the value with the highest selectivity is selected, regardless of the method from which the selectivity is obtained).[4] Color scheme: blue: calculated from multicomponent vapor-phase breakthrough experiments; red: calculated from vapor-phase sorption experiments; orange: calculated from chromatographic separation data; purple: calculated from batch solid–liquid sorption experiments; green: calculated using IAST based on vapor adsorption isotherms. More details are included in Table S4.

and pX/mX selectivities for corresponding binary equimolar mixtures were 378.8 and 860.5 at 120 °C and 1.2 Kpa, respectively (Figure S13–S16). To the best of our knowledge, these values are substantially higher than those of the reported adsorbents (Figure 2f)..[4–5,14–22] In addition, the adsorption capacity of pX by HIAM-203 (199 mg/g at 30 °C and 151 mg/g at 120 °C) is also higher than that of most representative adsorbents including Cu-metallocycle[22] (140 mg/g, 20 °C) and MFI zeolite[23] (131 mg/g, 25 °C), but slightly lower than that of Mn-dhbq (207 mg/g at 30 °C) which holds the record for pX-selective adsorbents.[4] To evaluate the cyclic performance of HIAM-203, three consecutive pX adsorption cycles at both 30 °C and 120 °C were collected (Figure S17–S18), The results indicated essentially no loss of adsorption capacity, suggesting good durability of the adsorbent.

The high adsorption selectivities of HIAM-203 as well as its high adsorption capacity suggested its great potential for the separation of xylene isomers. Multicomponent column breakthrough measurements were thus performed to evaluate the separation capability of the adsorbent. Breakthrough curves of pX/mX and pX/oX binary mixtures at 120 °C revealed mX or oX eluted out from the column at the very beginning of the measurements, suggesting they were fully excluded by the adsorbent (Figure 3a–3b). In contrast, pX was retained in the column for more than 250 minutes before its breakthrough. We further evaluated the separation ability of HIAM-203 for equimolar pX/mX/oX ternary mixture at both 30 and 120 °C. At 120 °C, mX and oX showed essentially no retention in the column while pX did not break out until the 327th minute (Figure 3c), yielding pX/oX and pX/mX selectivities of 211.2 and 171.9, respectively. This was consistent with the single-component adsorption results and confirmed that HIAM-203 is capable of discriminating pX/oX/mX isomers through selective molecular exclusion. Breakthrough results at 30 °C indicated the isomers could be separated as well, with slight retention for mX and oX which agreed well with the single-component adsorption results (Figure 3d).

To further evaluate the separation capability of HIAM-203 and compare its selective adsorption performance with benchmark adsorbents under similar conditions, multicomponent vapor-phase and liquid-phase adsorption experiments were performed at 120 °C following reported procedures.[4] The resultant pX/oX and pX/mX selectivities, along with the aforementioned selectivities calculated from IAST and breakthrough measurements are all higher than or similar to the previous records under similar conditions (Figure 2f and Table S4). These results confirmed the excellent performance of HIAM-203 for the separation of pX from its xylene isomers.

Ab initio calculations at the DFT level, using the vdW-DF functional, were carried out with the VASP code to further understand the adsorption dynamics and kinetics of

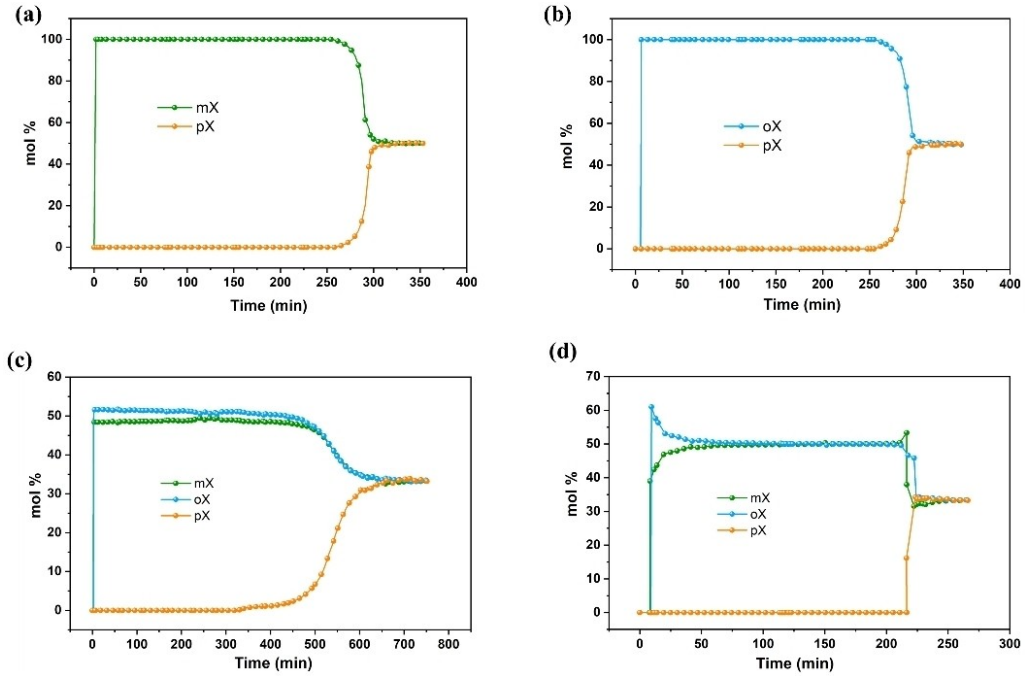

Figure 3. Breakthrough curves of an equimolar mixture of (a) pX /mX and (b) pX/oX at 120 °C. Breakthrough curves of an equimolar ternary mixture of xylene isomers at (c) 120 and (d) 30 °C for HIAM-203.

xylene isomers within HIAM-203.[24–29] The guest-free MOF structure was first relaxed and xylene isomers were subsequently loaded into HIAM-203 at various random positions inside the channel to find the optimum binding sites. All guest-loaded HIAM-203 systems were then further relaxed with the same optimization criteria. We found that all the xylene isomers induced noticeable changes in the framework depending on the size, morphology, and concentration of the guest molecules (Table S5). To investigate the interaction of xylene with HIAM-203, we calculated induced charge densities (i.e., the rearrangement of charge upon bond formation), showing a strong host–guest interaction. The xylene isomers mainly interact with the linkers including Cl atoms (see Figure S21). This strong interaction is also reflected in their binding energies of 1.627, 1.473, and 1.334 eV for pX, mX, and oX, respectively. In addition, we studied kinetic effects by calculating the energy barrier for guest molecules diffusing through the pores of HIAM-203. We observe that the energy barrier is closely related to the size of the guest molecules; the smaller the guest molecule, the lower the barrier. The energy barrier for pX is significantly smaller than the other two isomers thus giving the former a greater preference to be removed from the mixture (Figure 4). We also note that the framework flexibility/tilting of linkers as well as volume expansion play a crucial role and should be taken into account when modeling this system; we see a significant increase in the barrier heights when the cell internal coordinates were kept fixed.

In this work, we have demonstrated the unique advantages of a flexible MOF in separating xylene isomers by making use of its temperature- and adsorbate-dependent

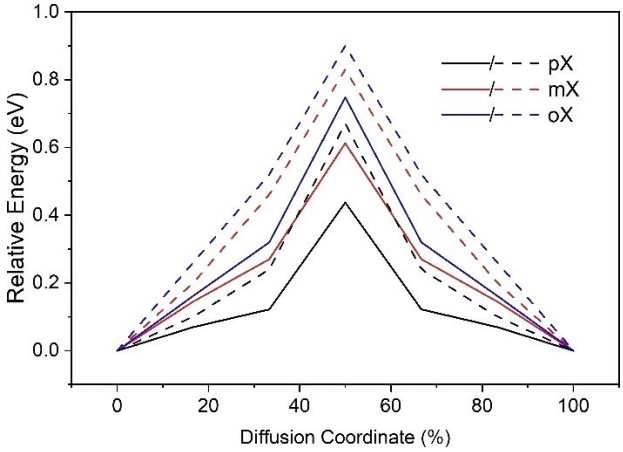

Figure 4. Energy barrier for xylene isomers during diffusion within HIAM-203. The solid/dashed lines represent variable/fixed cell transition-state calculations.

adsorption behavior. We show that HIAM-203, constructed on Ca^{2+} ion and chloranilate, exhibits distinct adsorption behaviors for xylene isomers. At 120 °C, it adsorbs pX but completely excludes its isomers mX and oX, thus behaving as a splitter for their separation. Its separation capability has been verified by single-component adsorption isotherms, adsorption kinetics, multicomponent column breakthrough measurements, multicomponent vapor-phase/liquid phase adsorption experiments, and ab initio calculations. The high and balanced adsorption selectivity and capacity of HIAM-203 suggest the great potential of designing flexible MOFs for challenging isomeric separations.

Acknowledgements

This work was financially supported by the National Natural Science Foundation of China (22178119), Shenzhen Science and Technology Program (No. RCYX20200714114539243, KCXFZ20211020163818026). Work in the U.S. was supported by the U.S. Department of Energy, Basic Energy Sciences, Division of Materials Sciences and Engineering (Grant No. DE-SC0019902). Computations were performed using the Wake Forest University High Performance Computing Facility, a centrally managed computational resource with support provided in part by the university.[30]

Conflict of Interest

The authors declare no conflict of interest.

Data Availability Statement

The data that support the findings of this study are available in the supplementary material of this article.

Keywords: Adsorptive Separation · Metal-Organic Frameworks · Size-Exclusion · Xylene Isomers

[1] "Separation of Xylene Isomers": J. Denayer, D. D. Vos, P. Leflaive, *Metal-Organic Frameworks: Applications from Catalysis to Gas Storage*, Wiley-VCH, Weinheim, **2011**.
[2] M. I. Gonzalez, M. T. Kapelewski, E. D. Bloch, P. J. Milner, D. A. Reed, M. R. Hudson, J. A. Mason, G. Barin, C. M. Brown, J. R. Long, *J. Am. Chem. Soc.* **2018**, *140*, 6921–6930.
[3] X. Li, J. Wang, N. Bai, X. Zhang, X. Han, I. da Silva, C. G. Morris, S. Xu, D. M. Wilary, Y. Sun, Y. Cheng, C. A. Murray, C. C. Tang, M. D. Frogley, G. Cinque, T. Lowe, H. Zhang, A. J. Ramirez-Cuesta, K. M. Thomas, L. W. Bolton, S. Yang, M. Schröder, *Nat. Commun.* **2020**, *11*, 4280.
[4] L. Li, L. Guo, D. H. Olson, S. Xian, Z. Zhang, Q. Yang, K. Wu, Y. Yang, Z. Bao, Q. Ren, J. Li, *Science* **2022**, *377*, 335–339.
[5] M. Rasouli, N. Yaghobi, F. Allahgholipour, H. Atashi, *Chem. Eng. Res. Des.* **2014**, *92*, 1192–1199.
[6] M. Lusi, L. J. Barbour, *Angew. Chem. Int. Ed.* **2012**, *51*, 3928–3931.
[7] A. M. Kałuża, S. Mukherjee, S. Q. Wang, D. J. O'Hearn, M. J. Zaworotko, *Chem. Commun.* **2020**, *56*, 1940–1943.
[8] X. Cui, Z. Niu, C. Shan, L. Yang, J. Hu, Q. Wang, P. C. Lan, Y. Li, L. Wojtas, S. Ma, H. Xing, *Nat. Commun.* **2020**, *11*, 5456.
[9] X. Yang, H. L. Zhou, C. T. He, Z. W. Mo, J. W. Ye, X. M. Chen, J. P. Zhang, *Research* **2019**, *2019*, 9463719.
[10] D. M. Polyukhov, A. S. Poryvaev, S. A. Gromilov, M. V. Fedin, *Nano Lett.* **2019**, *19*, 6506–6510.
[11] M. du Plessis, V. I. Nikolayenko, L. J. Barbour, *J. Am. Chem. Soc.* **2020**, *142*, 4529–4533.
[12] Y. Lin, L. Yu, S. Ullah, X. Li, H. Wang, Q. Xia, T. Thonhauser, J. Li, *Angew. Chem. Int. Ed.* **2022**, *61*, e202214060.
[13] Deposition number 2283986 contains the supplementary crystallographic data for this paper. These data are provided free of charge by the joint Cambridge Crystallographic Data Centre and Fachinformationszentrum Karlsruhe Access Structures service.
[14] D. Peralta, G. Chaplais, J. L. Paillaud, A. Simon-Masseron, K. Barthelet, G. D. Pirngruber, *Microporous Mesoporous Mater.* **2013**, *173*, 1–5.
[15] F. Vermoortele, M. Maes, P. Z. Moghadam, M. J. Lennox, F. Ragon, M. Boulhout, S. Biswas, K. G. Laurier, I. Beurroies, R. Denoyel, M. Roeffaers, N. Stock, T. Düren, C. Serre, D. E. De Vos, *J. Am. Chem. Soc.* **2011**, *133*, 18526–18529.
[16] M. Rasouli, N. Yaghobi, S. Z. Movassaghi Gilani, H. Atashi, M. Rasouli, *Chin. J. Chem. Eng.* **2015**, *23*, 64–70.
[17] J. E. Warren, C. G. Perkins, K. E. Jelfs, P. Boldrin, P. A. Chater, G. J. Miller, T. D. Manning, M. E. Briggs, K. C. Stylianou, J. B. Claridge, M. J. Rosseinsky, *Angew. Chem. Int. Ed.* **2014**, *53*, 4592–4596.
[18] N. Sun, S. Q. Wang, R. Zou, W. G. Cui, A. Zhang, T. Zhang, Q. Li, Z. Z. Zhuang, Y. H. Zhang, J. Xu, M. J. Zaworotko, X. H. Bu, *Chem. Sci.* **2019**, *10*, 8850–8854.
[19] K. Jie, M. Liu, Y. Zhou, M. A. Little, A. Pulido, S. Y. Chong, A. Stephenson, A. R. Hughes, F. Sakakibara, T. Ogoshi, F. Blanc, G. M. Day, F. Huang, A. I. Cooper, *J. Am. Chem. Soc.* **2018**, *140*, 6921–6930.
[20] B. Moosa, L. O. Alimi, A. Shkurenko, A. Fakim, P. M. Bhatt, G. Zhang, M. Eddaoudi, N. M. Khashab, *Angew. Chem. Int. Ed.* **2020**, *59*, 21367–21371.
[21] S. Mukherjee, B. Joarder, B. Manna, A. V. Desai, A. K. Chaudhari, S. K. Ghosh, *Sci. Rep.* **2014**, *4*, 5761.
[22] See Ref. [11]
[23] C. Long, *Microporous Mesoporous Mater.* **2000**, *39*, 149–161.
[24] G. Kresse, J. Furthmüller, *Phys. Rev. B* **1996**, *54*, 11169–11186.
[25] G. Kresse, D. Joubert, *Phys. Rev. B* **1999**, *59*, 1758–1775.
[26] T. Thonhauser, S. Zuluaga, C. A. Arter, K. Berland, E. Schröder, P. Hyldgaard, *Phys. Rev. Lett.* **2015**, *115*, 136402.
[27] D. C. Langreth, B. I. Lundqvist, S. D. Chakarova-Käck, V. R. Cooper, M. Dion, P. Hyldgaard, A. Kelkkanen, J. Kleis, L. Kong, S. Li, P. G. Moses, E. Murray, A. Puzder, H. Rydberg, E. Schröder, T. Thonhauser, *J. Phys. Condens. Matter* **2009**, *21*, 084203.
[28] K. Berland, V. R. Cooper, K. Lee, E. Schröder, T. Thonhauser, P. Hyldgaard, B. I. Lundqvist, *Rep. Prog. Phys.* **2015**, *78*, 066501.
[29] T. Thonhauser, V. R. Cooper, S. Li, A. Puzder, P. Hyldgaard, D. C. Langreth, *Phys. Rev. B* **2007**, *76*, 125112.
[30] I. Systems, W. F. University, **2021**.Information Systems and Wake Forest University, WFU High Performance Computing Facility, DOI: 10.57682/g13z-2362. (Please include the DOI, Thanks!)

Manuscript received: July 25, 2023
Accepted manuscript online: August 10, 2023
Version of record online: August 17, 2023